JOURNAL OF AIRCRAFT
Vol. 35, No. 5, September–October 1998

Airfoil Wave-Drag Prediction Using Euler Solutions of Transonic Flows

Christian Masson*
École de Technologie Supérieure, Montréal, Québec H3C 1K3, Canada
and
Charles Veilleux† and Ion Paraschivoiu‡
École Polytechnique de Montréal, Montréal, Québec H3C 3A7, Canada

The objective of the present work is the evaluation of four airfoil wave-drag prediction methods based on solutions of the Euler equations. In the case of two-dimensional inviscid flows of interest here, it is shown that the expression based on a volume integration of a positive definite quantity related to the artificial viscosity systematically underestimates the wave drag. In contrast with the popular belief, it is demonstrated that no clear improvement, in terms of accuracy, results from the use of far-field methods with respect to body-surface pressure integration. However, drag predictions obtained with entropy-based expression applied on a surface containing only the shocks are less sensitive to high levels of false entropy production because the drag contribution associated with false entropy production is eliminated. Furthermore, in three-dimensional flows, the wave and induced drag can be distinguished. A new method is proposed to correct the body-surface pressure integration estimates that is less sensitive to the level of false entropy production.

Nomenclature

C_{Dgar} = Garabedian wave-drag coefficient, Eq. (20)
C_{Dm} = momentum-flux drag coefficient, Eq. (14)
C'_{Dm} = C_{Dm} with artificial viscosity contributions, Eq. (15)
C_{Dosw} = Oswatitsch wave-drag coefficient, Eq. (18)
$C_{Dosw|_{shock}}$ = Oswatitsch wave-drag coefficient integrated on the shock, Eq. (19)
C_{Dp} = pressure drag coefficient, Eq. (13)
C_{Dp}^{corr} = corrected body-surface pressure integration coefficient, Eq. (21)
C_{Ds} = exact Oswatitsch wave-drag coefficient, Eq. (16)
$C_{Ds|_{shock}}$ = exact Oswatitsch wave-drag coefficient integrated on the shock, Eq. (17)
c = airfoil chord
c_v = constant-volume specific heat
D = total drag
dS = differential surface
e = specific internal energy
$\boldsymbol{i}$ = unit vector in freestream direction
M_∞ = freestream Mach number
$\boldsymbol{n}$ = unit outward vector normal to dS
p = pressure
$\boldsymbol{q}$ = velocity vector
R = ideal gas constant
r = distance between the body surface and the integration surface, Fig. 3a
S = integration surface in the far field enclosing the body
S_B = body surface
S_{shock} = integration surface enclosing the vicinity of the shocks
s = specific entropy
U_∞ = freestream velocity
u = velocity component in the freestream direction
$\|w\|^2_{WD}$ = positive definite quantity, Eq. (9)
α = angle of attack
γ = specific heat ratio
μ = artificial viscosity
ρ = density
τ = artificial viscous stress tensor

Subscript
∞ = freestream value

Received Nov. 3, 1997; revision received May 15, 1998; accepted for publication May 27, 1998.

*Associate Professor, Mechanical Engineering Department. Member AIAA.
†Propulsion Specialist, Mechanical Engineering Department; currently at CAE Electronics Ltd., Ville St-Laurent, Québec H4L 4X4, Canada.
‡Chair Professor, J.-A. Bombardier Aeronautical Chair. Associate Fellow AIAA.

Introduction

IN the field of aircraft design, accurate prediction of drag is an essential requirement for performance predictions as well as fuel consumption reduction. During a drag-reduction procedure, an evaluation of the total drag of a wing by the body-surface integration of pressure and viscous shear is not sufficient. The total drag must be evaluated in terms of its components (boundary layer, induced, and wave drags) to identify the source of abnormally high drag production.

In this work, various methods for the evaluation of the wave drag are presented and implemented for airfoils. The first method involves Oswatitsch's drag expression,[1] relating wave drag to the rate of entropy production through the shock waves. An integration of the rate of entropy production on a closed surface enclosing the body yields the wave drag. Two types of surfaces are considered: surfaces enclosing the body and a suitable surface enclosing only the shocks. The second method involves Garabedian's volume integration,[2,3] developed from the entropy inequality that is fundamental to the method of artificial viscosity. This method relates the rate of entropy production to the explicit artificial viscosity terms typically introduced in inviscid flow solvers and, thus, transforms the far-field surface integration of the rate of entropy production to a volume integration of a positive definite quantity over the entire calculation domain. The wave drag is also evaluated from integration of the body-surface pressure and by a far-field momentum-flux integration.

Inviscid Flow Calculations

The two-dimensional Euler solver used in this work is a finite volume cell-centered scheme with second- and fourth-

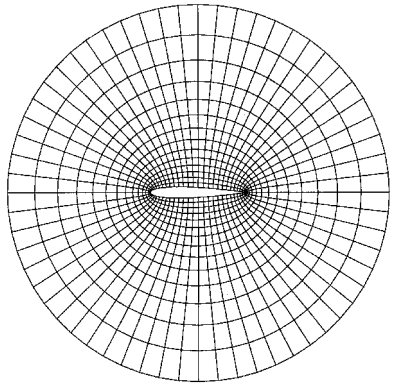

Fig. 1 Typical O-grid used to discretize the calculation domain.

order artificial viscosity.[4] The governing equations are integrated in time using a fifth-order Runge–Kutta time-stepping scheme. A structured O-grid is used to discretise the calculation domain (see Fig. 1). This Euler solver is similar to a wide range of solvers used in the aircraft community. It is to be noted that the conclusions and recommendations of this work apply to any conservative Euler solver.

Wave-Drag Calculations

In inviscid flow, the total drag D acting on a body results from the pressure distribution over S_B, and is given by the following body-surface integral:

$$D = \int_{S_B} -p\boldsymbol{n}\cdot\boldsymbol{i}\,\mathrm{d}S \tag{1}$$

For the two-dimensional inviscid flows of interest here, the total drag of Eq. (1) is the wave drag, and the surface integral reduces to a contour integral. For the evaluation of the profile drag, which is the sum of the surface friction drag and the boundary-layer pressure drag, viscous/inviscid solutions or Navier–Stokes solutions must be analyzed. This is the expression most commonly used for the evaluation of the drag and it will be referred to as the "body-surface pressure integration" in this work. The drag coefficient computed using this expression will be denoted C_{Dp}.

A far-field expression for the drag can be derived using the momentum equations applied on any control volume enclosing the body of interest:

$$D = -\int_S (p\boldsymbol{n}\cdot\boldsymbol{i} + \rho u\boldsymbol{q}\cdot\boldsymbol{n})\,\mathrm{d}S \tag{2}$$

Equation (2) relates the drag to a far-field momentum-flux integral. The drag coefficient calculated using this momentum-flux integral will be denoted C_{Dm}.

Oswatitsch's Expression

Oswatitsch has derived an approximate expression relating the wave drag to the rate of entropy production in a steady adiabatic inviscid flow of an ideal gas.[1] In such a flow, it is possible to relate the momentum deficit to the rate of entropy production using the following procedure.

First, using the conservation of mass principle over the control volume, the far-field expression for the drag of a body [Eq. (2)] can be expressed as

$$D = -\int_S \left[(p - p_\infty)\boldsymbol{n}\cdot\boldsymbol{i} - U_\infty\left(1 - \frac{u}{U_\infty}\right)\rho\boldsymbol{q}\cdot\boldsymbol{n}\right]\mathrm{d}S \tag{3}$$

Assuming the fluid to be an ideal gas and the flow to be adiabatic, the expression of the conservation of the energy can be expressed as

$$\left(\frac{q}{U_\infty}\right)^2 = 1 + \frac{2}{(\gamma-1)M_\infty^2}\left\{1 - \left[\frac{p}{p_\infty}\exp\left(\frac{s-s_\infty}{R}\right)\right]^{[(\gamma-1)/\gamma]}\right\} \tag{4}$$

When the surface of integration S is sufficiently far from the body, the only significant component of the velocity vector is u, $p \approx p_\infty$, and we can obtain the following expression:

$$\left(1 - \frac{u}{U_\infty}\right) \approx \left(1 - \frac{q}{U_\infty}\right) = 1 - \sqrt{1 + \frac{2}{(\gamma-1)M_\infty^2}\left\{1 - \exp\left[\left(\frac{s-s_\infty}{R}\right)\left(\frac{\gamma-1}{\gamma}\right)\right]\right\}} \tag{5}$$

Finally, introducing Eq. (5) in Eq. (3) yields

$$D = \int_S U_\infty\left[1 - \sqrt{1 + \frac{2}{(\gamma-1)M_\infty^2}\left\{1 - \exp\left[\left(\frac{s-s_\infty}{R}\right)\left(\frac{\gamma-1}{\gamma}\right)\right]\right\}}\right]\rho\boldsymbol{q}\cdot\boldsymbol{n}\,\mathrm{d}S \tag{6}$$

This equation is based on the exact relation between entropy production and wave drag in inviscid flows and will be referred to as the exact Oswatitsch's expression. The drag coefficient computed with this expression will be denoted C_{Ds}. It is to be noted that this equation is valid only when there is no powered engines within the closed surface S. An extension of this expression, when powered engines are included, has been presented by Cummings et al.[5] Furthermore, the Oswatitsch expression, and any other entropy-based expressions, are not applicable to isentropic solutions such as those produced by the full-potential equation. In such flows, a specific formula has been derived[6] that relates the wave drag to the momentum gain through the isentropic shock.

The surface of integration S used to derive this expression was assumed to enclose the body and to be far from it. However, any surface of integration that encloses only the immediate vicinity of the shock waves can be used because the entropy changes occur only through the shocks and $\boldsymbol{q}\cdot\boldsymbol{n} = 0$ on S_B. When a surface of integration enclosing only the immediate vicinity of the shocks is used to compute the drag based on the exact Oswatitsch's expression, the drag coefficient will be denoted $C_{\mathrm{Ds}|_{\mathrm{shock}}}$.

Expansion of the integrand of Eq. (6) to the lowest order in $(s - s_\infty)$ leads to the so-called "approximate Oswatitsch's expression"

$$D = \frac{U_\infty}{\gamma R M_\infty^2}\int_S (s - s_\infty)\rho\boldsymbol{q}\cdot\boldsymbol{n}\,\mathrm{d}S \tag{7}$$

The drag coefficient computed by applying Oswatitsch's expression[1] on an integration surface enclosing the body will be denoted C_{Dosw}. When S in Eq. (7) encloses only the shock waves, the drag coefficient will be denoted $C_{\mathrm{Dosw}|_{\mathrm{shock}}}$.

Garabedian's Volume Integration

Garabedian[2] proposed an alternative way of calculating wave drag based on a volume integration over the entire flowfield. In this method, the rate of entropy production is related to the explicit artificial viscosity typically introduced in inviscid flow solvers and, thus, the far-field surface integration of

the rate of entropy production, derived by Oswatitsch [see Eq. (7)], is transformed into a volume integration of a positive definite quantity related to the artificial viscosity over the entire calculation domain.

Assuming steady-state flows and neglecting the fourth-order artificial viscosity terms introduced in the Euler equations, an expression relating entropy production and artificial viscosity can be derived[2,3]

$$\nabla \cdot \rho s \boldsymbol{q} = \frac{c_v \rho}{e} \|w\|^2_{WD} + \nabla \cdot \mu \left(s \nabla \rho + \frac{c_v \rho \nabla e}{e} + \frac{c_v \nabla p}{e} \right) \quad (8)$$

where

$$\|w\|^2_{WD} = \|\nabla u\|^2 + \|\nabla v\|^2 + \gamma e \left(\left\| \frac{\nabla p}{p} \right\|^2 - \frac{\gamma + 1}{\gamma} \left\| \frac{\nabla p}{p}, \frac{\nabla \rho}{\rho} \right\| + \left\| \frac{\nabla \rho}{\rho} \right\|^2 \right) \quad (9)$$

with, for example

$$\|w\|^2 = \|w, w\| \text{ and } \left\| \frac{\nabla p}{p}, \frac{\nabla \rho}{\rho} \right\| = \frac{\nabla p^T}{p} \mu \frac{\nabla \rho}{\rho}$$

Equation (8) may be integrated over the flow domain V. If V is the entire flow domain, the left-hand side of Eq. (8) reduces to an integration at the outer surface S because $\boldsymbol{q} \cdot \boldsymbol{n} = 0$ on S_B, and the second integral on the right-hand side may be neglected.[3] Thus

$$\int_S \rho s \boldsymbol{q} \cdot \boldsymbol{n} \, dS = \int_V \frac{c_v \rho}{e} \|w\|^2_{WD} \, dV \quad (10)$$

Using the integral expression of the conservation of mass, one can easily show that

$$\int_S \rho s \boldsymbol{q} \cdot \boldsymbol{n} \, dS = \int_S \rho (s - s_\infty) \boldsymbol{q} \cdot \boldsymbol{n} \, dS \quad (11)$$

This last expression can be combined with Eqs. (7) and (10) to give

$$D = \frac{U_\infty}{\gamma R M^2_\infty} \int_V \frac{c_v \rho}{e} \|w\|^2_{WD} \, dV \quad (12)$$

which is the expression between the wave drag and the volume integration of a positive definite quantity related to the artificial viscosity ($\|w\|^2_{WD}$). It will be referred to as "Garabedian's volume integration." The drag coefficient calculated using Eq. (12) will be denoted C_{Dgar}. Details concerning the derivation of this expression can be found in Ref. 3.

Results and Discussion

The results presented in this section pertain to the inviscid, compressible flow over a NACA 0012 airfoil. The drag expressions developed in the previous section have been implemented in the Euler solver described previously. More specifically, the following eight expressions have been used:

$$C_{Dp} = \frac{1}{1/2 \rho_\infty U^2_\infty c} \int_{S_B} -p \boldsymbol{n} \cdot \boldsymbol{i} \, dS \quad (13)$$

$$C_{Dm} = \frac{1}{1/2 \rho_\infty U^2_\infty c} \int_S (-p \boldsymbol{n} \cdot \boldsymbol{i} - \rho u \boldsymbol{q} \cdot \boldsymbol{n}) \, dS \quad (14)$$

$$C'_{Dm} = C_{Dm} + \frac{1}{1/2 \rho_\infty U^2_\infty c} \int_S (\tau \cdot \boldsymbol{n}) \cdot \boldsymbol{i} \, dS \quad (15)$$

$$C_{Ds} = \frac{1}{1/2 \rho_\infty U^2_\infty c} U_\infty \int_S \left(1 - \sqrt{1 + \frac{1}{(\gamma - 1) M^2_\infty} \left\{ 1 - \exp \left[\left(\frac{s - s_\infty}{R} \right) \left(\frac{\gamma - 1}{\gamma} \right) \right] \right\}} \right) \rho \boldsymbol{q} \cdot \boldsymbol{n} \, dS \quad (16)$$

$$C_{Ds|_{shock}} = \frac{1}{1/2 \rho_\infty U^2_\infty c} U_\infty \int_{S_{shock}} \left(1 - \sqrt{1 + \frac{2}{(\gamma - 1) M^2_\infty} \left\{ 1 - \exp \left[\left(\frac{s - s_\infty}{R} \right) \left(\frac{\gamma - 1}{\gamma} \right) \right] \right\}} \right) \rho \boldsymbol{q} \cdot \boldsymbol{n} \, dS \quad (17)$$

$$C_{Dosw} = \frac{1}{1/2 \rho_\infty U^2_\infty c} \frac{U_\infty}{\gamma R M^2_\infty} \int_S (s - s_\infty) \rho \boldsymbol{q} \cdot \boldsymbol{n} \, dS \quad (18)$$

$$C_{Dosw|_{shock}} = \frac{1}{1/2 \rho_\infty U^2_\infty c} \frac{U_\infty}{\gamma R M^2_\infty} \int_{S_{shock}} (s - s_\infty) \rho \boldsymbol{q} \cdot \boldsymbol{n} \, dS \quad (19)$$

$$C_{Dgar} = \frac{1}{1/2 \rho_\infty U^2_\infty c} \frac{U_\infty}{\gamma R M^2_\infty} \int_V \frac{c_v \rho}{e} \|w\|^2_{WD} \, dV \quad (20)$$

In these expressions, S, the contour enclosing the body, is taken as the contour defined by a specific O-line of the grid used to produce the Euler solutions (see Fig. 1). Drag coefficient calculations have been performed for each O-line, from the body surface to the outer surface of the calculation domain. S_{shock} is a contour enclosing only the immediate vicinity of the shocks to eliminate the false-entropy drag contribution typically observed near the stagnation point. The drag coefficient that includes both the momentum and artificial viscous stress contributions, C'_{Dm}, has been implemented to quantify the relative importance of the artificial viscous stresses in the flow.

Because the flow solver is based on a conservative formulation, the drag coefficient based on the body-surface pressure integration (C_{Dp}) should be exactly equal to C'_{Dm}. This is indeed the case with the Euler solutions presented in this section. Therefore, the values of C_{Dp} and C'_{Dm} are indistinguishable in all of the figures presented in this paper. In regions where the artificial viscous stresses are negligible, C_{Dm} should also be very close to C_{Dp}.

Drag predictions using Eqs. (16–20) largely rely on the quality of the solution with respect to the entropy distribution. Figure 2a illustrates typical entropy distributions produced by the two-dimensional Euler solver used in this work. False entropy production is noted in the vicinity of the body surface and, more specifically, near the stagnation point (see Fig. 2b).

Figure 3a shows the variation of the eight drag estimates with respect to S, the chosen surface of integration enclosing the airfoil, characterized by its radial distance r from the body surface. The values of $C_{Ds|_{shock}}$ and $C_{Dosw|_{shock}}$ are calculated on an integration surface that encloses only the immediate vicinity of the shocks. Therefore, these drag estimates are not functions of r/c, so that they are presented as constant in Fig. 3a. In this figure C_{Dgar} is given in the legend because its value lies outside of the illustrated scale. In fact, as the freestream Mach number increases, it has been observed that Garabedian's volume integration leads to significantly lower wave-drag estimates than the predictions based on the other expressions (see Table 1).

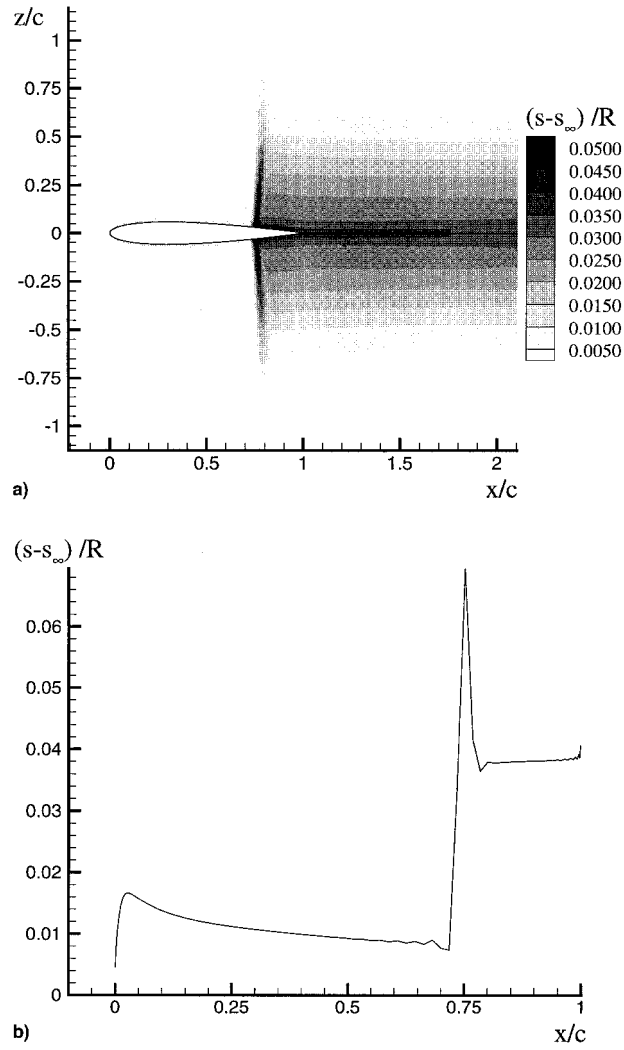

Fig. 2 $M_\infty = 0.85, \alpha = 0.00, 160 \times 40$ O-grid: a) entropy contours and b) surface distribution.

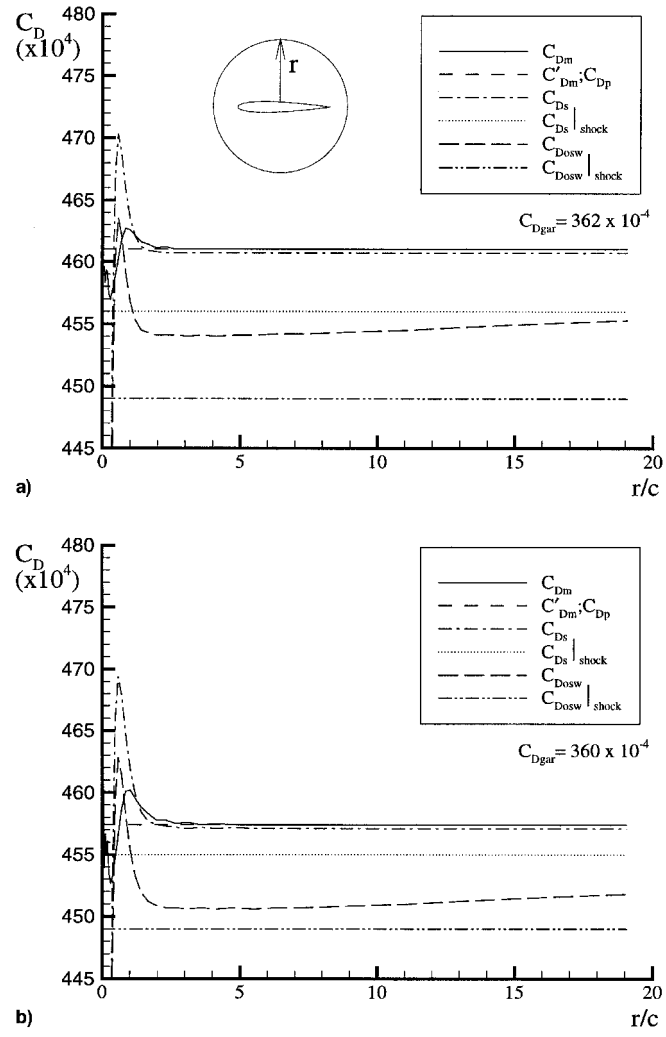

Fig. 3 Drag predictions based on different integration contours —$M_\infty = 0.85, \alpha = 0.00, 160 \times 40$ O-grid: a) without and b) with weighting function.

A remarkable behavior illustrated in Fig. 3a is the fact that when the chosen integration surface is far enough from the body ($r/c > 4$), the values of C_{Dp}, C_{Dm}, C'_{Dm}, and C_{Ds} are essentially constant and in very good agreement with one another.

The values of C_{Ds} and C_{Dosw} vary for $r/c < 4$ because the integration surface does not enclose the shocks completely. The difference between C'_{Dm} and C_{Dm}, again noted for $r/c < 4$, is produced by the artificial viscous stress contribution.

The drag estimate based on Oswatitsch's expression, C_{Dosw}, is lower than the previously noted unique value of C_{Dp}, C_{Dm}, and C'_{Dm}. This discrepancy is attributed to the first-order approximation in $(s - s_\infty)$ introduced to obtain Eq. (7). This approximation produces an error that grows with M_∞. At lower freestream Mach numbers, the difference between the drag estimate based on C_{Ds} and C_{Dosw} tends to zero (see Fig. 4a). At such low freestream Mach numbers, the four drag estimates C_{Dm}, C'_{Dm}, D_{Ds}, and C_{Dosw} are essentially equal (see Table 1).

The very good agreement between the drag estimates C_{Dp}, C_{Dm}, C'_{Dm}, and C_{Ds} clearly indicates that no significant improvement, in terms of accuracy, results from the use of a far-field approach with respect to a simple body-surface pressure integration. Similar conclusions have been drawn by Varma and Caughey[7] in the context of two-dimensional Navier–Stokes solutions. Nevertheless, many researchers attribute the poor results obtained with body-surface pressure integration to the discretization of the body surface into panels: the pressure integration was thought to be less accurate on this surface leading to unsatisfactory pressure coefficients, particularly with coarser grids.[8–10] In fact, the discrepancies noted between the pressure coefficient and the far-field coefficients are caused by the false entropy production near the stagnation point generally produced by Euler flow solvers.

Integration of the rate of entropy production on a surface enclosing only the immediate vicinity of the shocks, $C_{Ds|_{shock}}$ and $C_{Dosw|_{shock}}$, produces drag estimates that are lower than the essentially unique value of C_{Dp}, C_{Dm}, C'_{Dm}, and C_{Ds} because such surface of integration allows removal of the drag contribution associated with false entropy production near the stagnation point. In fact, it is this capacity to eliminate the false entropy production contribution that represents the main advantage of drag calculation methods based on the integration of the rate of entropy production. Furthermore, in three-dimensional inviscid flows (not considered here), such entropy-based drag predictions allows one to distinguish the wave drag from the induced drag. In contrast, only the total drag is computed using body-surface pressure integration or far-field momentum-flux integration, when analyzing three-dimensional inviscid flows.

Yu et al.[11] mentioned that the false entropy production is mainly caused by inaccurate calculation of the artificial dissipation terms at the body surface, and proposed to apply a weighting function to scale the viscous dissipation terms in the normal direction so that they are gradually turned on from the body surface to the far field. The effects of this enhancement on drag prediction are illustrated in Figs. 3b and 4b. It is seen

Table 1 Summary of drag predictions, 160 × 40 O-grid

		Present solution $C_D(\times 10^4)$								
M_∞	α deg	C_{Dp}	C_{Dm}	C'_{Dm}	C_{Ds}	$C_{Ds\|_{shock}}$	C_{Dosw}	$C_{Dosw\|_{shock}}$	C_{Dgar}	C_{Dp}^{corr}
0.74	0.00	6	6	6	6	0	6	0	3	0
0.76	0.00	9	9	9	9	4	9	4	5	4
0.78	0.00	30	30	30	30	25	30	25	22	25
0.80	0.00	89	89	89	89	84	89	84	69	84
0.82	0.00	197	197	197	197	192	196	190	155	192
0.85	0.00	461	461	461	461	456	455	449	362	456

Table 2 Effects of grid refinement on drag predictions, $M_\infty = 0.85$, $\alpha = 0.00$

	Present solution $C_D(\times 10^4)$								
O-grid	C_{Dp}	C_{Dm}	C'_{Dm}	C_{Ds}	$C_{Ds\|_{shock}}$	C_{Dosw}	$C_{Dosw\|_{shock}}$	C_{Dgar}	C_{Dp}^{corr}
160 × 40	461	461	461	461	456	455	449	362	456
128 × 32	469	469	469	469	462	463	455	367	462
80 × 20	486	486	486	486	470	480	463	379	470

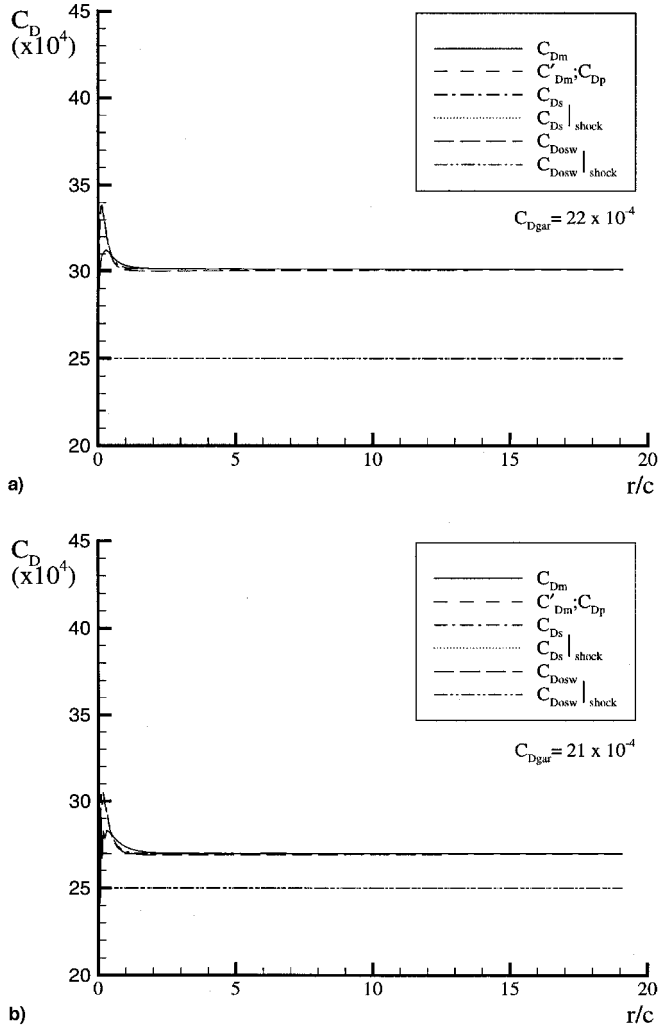

Fig. 4 Drag predictions based on different integration contours —$M_\infty = 0.78$, $\alpha = 0.00$, 160 × 40 O-grid: a) without and b) with weighting function.

that the drag contribution associated to false entropy production, represented by the differences $(C_{Ds} - C_{Ds|_{shock}})$ and $(C_{Dosw} - C_{Dosw|_{shock}})$, is reduced when such weighting is applied. In the present work, only the results presented in Figs. 3b and 4b have been obtained using this enhancement. Ultimately, if all false entropy production in the flowfield could be eliminated, the drag coefficients C_{Dp}, C_{Dm}, C'_{Dm}, C_{Ds}, and $C_{Ds|_{shock}}$ would be equal so that any of these methods would be equivalent.

The behavior of the various drag estimates with respect to grid refinement is presented in Table 2. It has been observed that the false entropy production increases with coarser grids. This behavior leads to higher estimates of drag on coarse grids compared to fine ones. A correction procedure can be proposed for the body-surface pressure coefficient that could be useful, particularly on coarse grids. The difference $(C_{Ds} - C_{Ds|_{shock}})$ gives an indication of the contribution of the false entropy to the total drag C_{Dp}. A corrected body-surface pressure integration coefficient C_{Dp}^{corr} is given by

$$C_{Dp}^{corr} = C_{Dp} - (C_{Ds} - C_{Ds|_{shock}}) \simeq C_{Ds|_{shock}} \tag{21}$$

The corrected pressure coefficients are given in the last column of Tables 1 and 2. These estimates are clearly less sensitive to the level of false entropy production and are in perfect agreement with the $C_{Ds|_{shock}}$ estimates.

Conclusions

In this work, eight different techniques for the evaluation of the wave drag have been presented and implemented for airfoils. These various techniques have been derived from the application of Oswatitsch's expression[1], Garabedian's volume integration[2], body-surface pressure integration, and far-field momentum-flux integration. Results are presented for the inviscid compressible flow over a NACA 0012 airfoil. It has been shown that the application of Garabedian's volume integration leads to significantly lower wave-drag estimates than the predictions based on the other expressions. In contrast with popular belief, it is demonstrated that, for two-dimensional inviscid flows considered in this paper, there is no advantage, in terms of accuracy, of using far-field methods. No significant differences are noted among the drag predictions based on Oswatitsch's expression, a momentum-flux integral, and a simple body-surface pressure integration, provided appropriate integration surfaces are selected and false entropy production near the body surface is negligible. However, drag prediction methods based on the integration of the rate of entropy production, such as Oswatitch's expression, allow the distinction of the wave drag and induced drag in three-dimensional flows. In contrast, only the total drag is computed using body-surface pressure integration or far-field momentum-flux integration, when analyzing three-dimensional inviscid flows. Drag predictions based on Oswatitsch's expression applied on a surface containing only the shocks are less sensitive to high levels of false entropy production because the drag contribution associated with false entropy production is eliminated. A method was proposed to improve the accuracy of the body-surface

pressure integration estimates that is less sensitive to the level of false entropy production.

Acknowledgments

This work is supported by a Natural Sciences and Engineering Research Council of Canada (NSERC) collaborative Research and Development Grant with Bombardier Inc./Canadair. The support of NSERC and Fonds pour la Formation de Chercheurs et l'Aide à la Recherche in the form of research grants to the first author is gratefully acknowledged.

References

[1]Oswatitsch, K., *Gas Dynamics*, Academic, New York, 1956.

[2]Garabedian, P. R., "Computation of Wave Drag for Transonic Flow," *Journal d'Analyse Mathématique*, Vol. 30, 1976, pp. 164–171.

[3]McGrattan, K., "Comparison of Transonic Flow Models," *AIAA Journal*, Vol. 30, No. 9, 1992, pp. 2340–2343.

[4]Jameson, A., Schmidt, W., and Turkel, E., "Numerical Solutions of the Euler Equations by Finite Volume Methods Using Runge-Kutta Time-Stepping Schemes," AIAA Paper 81-1259, June 1981.

[5]Cummings, R. M., Giles, M. B., and Shrinivas, G. N., "Analysis of the Drag in Three-Dimensional Viscous and Inviscid Flows," AIAA Paper 96-2482, June 1996.

[6]Steger, J. L., and Barrett, S. B., "Shock Waves and Drag in the Numerical Calculation of Isentropic Transonic Flow," NASA TN D-6997, Oct. 1972.

[7]Varma, R. R., and Caughey, D. A., "Evaluation of Navier-Stokes Solutions Using the Integrated Effects of Numerical Dissipation," *AIAA Journal*, Vol. 32, No. 2, 1994, pp. 294–300.

[8]Janus, J. M., and Chatterjee, A., "Use of a Wake-Integral Method for Computational Drag Analysis," *AIAA Journal*, Vol. 34, No. 1, 1995, pp. 188–190.

[9]Cummings, R. M., Giles, M. B., and Shrinivas, G. N., "Analysis of the Elements of Drag in Three-Dimensional Viscous and Inviscid Flows," AIAA Paper 96-2482, June 1996.

[10]Van Dam, C. P., and Nikfetrat, K., "Accurate Prediction of Drag Using Euler Methods," *Journal of Aircraft*, Vol. 29, No. 3, 1991, pp. 516–519.

[11]Yu, N. J., Chen, H. C., Samant, S. S., and Ruppert, P. E., "Inviscid Drag Calculations for Transonic Flows," AIAA Paper 83-1928, July 1983.